HYDROTHERMAL ANALYSIS IN ENGINEERING USING CONTROL VOLUME FINITE ELEMENT METHOD

Mohsen Sheikholeslami Kandelousi
Davood Domairry Ganji

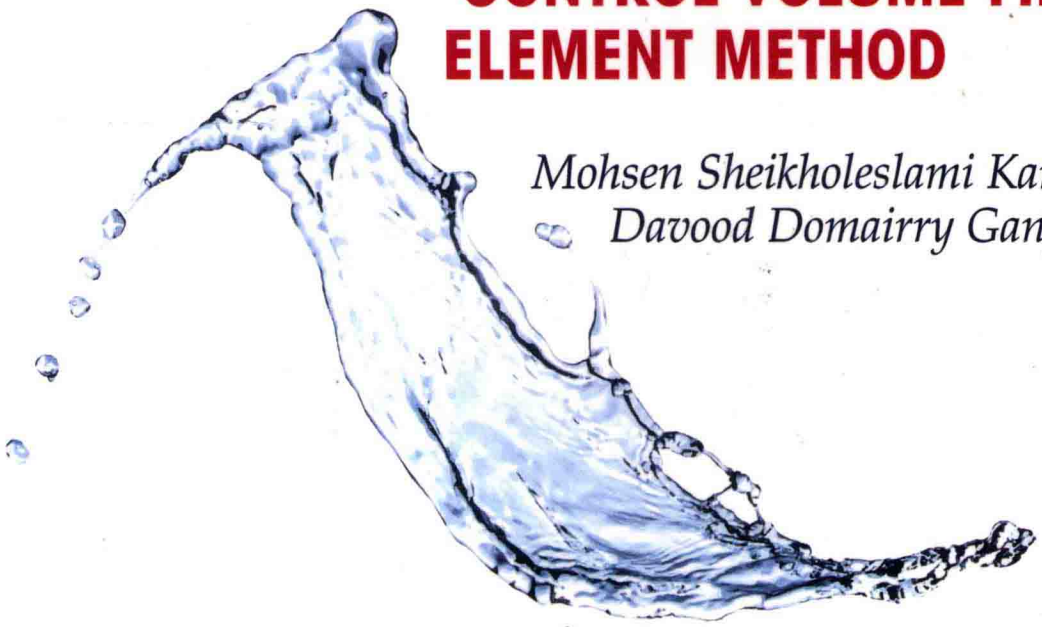

Hydrothermal Analysis in Engineering Using Control Volume Finite Element Method

Mohsen Sheikholeslami Kandelousi
Department of Mechanical Engineering,
Babol University of Technology

Davood Domairry Ganji
Department of Mechanical Engineering,
Babol University of Technology

ELSEVIER

AMSTERDAM • BOSTON • HEIDELBERG • LONDON
NEW YORK • OXFORD • PARIS • SAN DIEGO
SAN FRANCISCO • SINGAPORE • SYDNEY • TOKYO
Academic Press is an imprint of Elsevier

Academic Press is an imprint of Elsevier
125, London Wall, EC2Y 5AS
525 B Street, Suite 1800, San Diego, CA 92101-4495, USA
225 Wyman Street, Waltham, MA 02451, USA
The Boulevard, Langford Lane, Kidlington, Oxford OX5 1GB, UK

Notices

Knowledge and best practice in this field are constantly changing. As new research and experience broaden our understanding, changes in research methods, professional practices, or medical treatment may become necessary.

Practitioners and researchers must always rely on their own experience and knowledge in evaluating and using any information, methods, compounds, or experiments described herein. In using such information or methods they should be mindful of their own safety and the safety of others, including parties for whom they have a professional responsibility.

To the fullest extent of the law, neither the Publisher nor the authors, contributors, or editors, assume any liability for any injury and/or damage to persons or property as a matter of products liability, negligence or otherwise, or from any use or operation of any methods, products, instructions, or ideas contained in the material herein.

British Library Cataloguing in Publication Data
A catalogue record for this book is available from the British Library

Library of Congress Cataloging-in-Publication Data
A catalog record for this book is available from the Library of Congress

ISBN: 978-0-12-802950-3

Hydrothermal Analysis in Engineering Using Control Volume Finite Element Method

Preface

In this book we provide readers with the fundamentals of the control volume finite element method (CVFEM) for heat and fluid flow problems. The CVFEM comprises interesting characteristics of both the finite volume and finite element methods. It combines the flexibility of the finite element methods to discretize complex geometry with the conservative formulation of the finite volume methods, in which variables can be easily interpreted physically in terms of fluxes, forces, and sources. Most other available texts concentrate on solids problems. We applied this method for flow and heat transfer. Application of CVFEM in different interesting fields such as nanofluid flow and heat transfer, magnetohydrodynamics, ferrohydrodynamics, and porous media is considered. Several examples have been prepared in these fields of science. This text is suitable for senior undergraduate students, postgraduate students, engineers, and scientists.

The first chapter of the book deals with the essential fundamentals of the CVFEM. The necessary ingredients in numerical solutions are discussed. Chapter 2 deals with solving Navier-Stokes equations (in vorticity stream function form) and energy equations. In this chapter two basic important problems are solved via the CVFEM. The third chapter gives a complete account of the nanofluid hydrothermal behavior and application of CVFEM to solve such problems. All the relevant differential equations are derived from first principles. All three types of convection modes—forced, mixed, and natural convection—are discussed in detail. Examples and comparisons are provided to support the accuracy and flexibility of the CVEFM. Examples start with a single-phase model and then extend to a two-phase model.

The application of the CVEFM to heat and fluid flow in the presence of a magnetic field are discussed in detail in Chapter 4. Two kinds of magnetic fields are considered: a constant magnetic field and a spatially variable magnetic field. Several examples included in Chapter 4 give the reader a full account of the theory and practice associated with the CVFEM. Chapter 5 gives the procedures for solving equations of flow and heat transfer in porous media. Some examples provide readers with an opportunity to learn about the effect of active parameters. A sample FORTRAN code for advection-diffusion in lid-driven cavity geometry is presented in Appendix. Readers will be able to extend this code and solve all of the examples within this book.

Mohsen Sheikholeslami Kandelousi
Davood Domairry Ganji

Contents

Nomenclature vii
Preface ix

CHAPTER 1 Control Volume Finite Element Method (CVFEM) 1

1.1 Introduction 1
1.2 Discretization: Grid, Mesh, and Cloud 1
1.2.1 Grid 2
1.2.2 Mesh 2
1.2.3 Cloud 3
1.3 Element and Interpolation Shape Functions 3
1.4 Region of Support and Control Volume 5
1.5 Discretization and Solution 6
1.5.1 Steady-State Advection-Diffusion with Source Terms 6
1.5.2 Implementation of Source Terms and Boundary Conditions 8
1.5.3 Unsteady Advection-Diffusion with Source Terms 9
References 11

CHAPTER 2 CVFEM Stream Function-Vorticity Solution 13

2.1 CVFEM Stream Function-Vorticity Solution for a Lid-Driven Cavity Flow 13
2.1.1 Definition of the Problem and Governing Equation 13
2.1.2 The CVFEM Discretization of the Stream Function Equation 14
2.1.3 The CVFEM Discretization of the Vorticity Equation 16
2.1.4 Calculating the Nodal Velocity Field 18
2.1.5 Results 19
2.2 CVFEM Stream Function-Vorticity Solution for Natural Convection 19
2.2.1 Definition of the Problem and Governing Equation 19
2.2.2 Effect of Active Parameters 21
References 30

CHAPTER 3 Nanofluid Flow and Heat Transfer in an Enclosure 31

3.1 Introduction 31
3.2 Nanofluid 34
3.2.1 Definition of Nanofluid 34
3.2.2 Model Description 34

3.2.3 Conservation Equations 34
3.2.4 Physical Properties of Nanofluids in a Single-Phase Model 38
3.3 Simulation of Nanofluid in Vorticity Stream Function form 40
3.3.1 Mathematical Modeling of a Single-Phase Model 40
3.3.2 CVFEM for Nanofluid Flow and Heat Transfer (Single-Phase Model) 44
3.3.3 Two-Phase Model 57
3.3.4 CVFEM for Nanofluid Flow and Heat Transfer (Two-Phase Model) 60
References 72

CHAPTER 4 Flow Heat Transfer in the Presence of a Magnetic Field 77

4.1 Introduction 77
4.2 MHD Nanofluid Flow and Heat Transfer 79
4.2.1 Mathematical Modeling for a Single-Phase Model 80
4.2.2 Mathematical Modeling for a Two-Phase Model 83
4.2.3 Application of the CVFEM for MHD Nanofluid Flow and Heat Transfer 85
4.3 Combined Effects of Ferrohydrodynamics and MHD 141
4.3.1 Mathematical Modeling for a Single-Phase Model 142
4.3.2 Mathematical Modeling for a Two-Phase Model 146
4.3.3 Application of CVFEM for the Combined Effects of FHD and MHD 149
References 174

CHAPTER 5 Flow and Heat Transfer in Porous Media 177

5.1 Introduction 177
5.2 Governing Equations for Flow and Heat Transfer in Porous Media 178
5.3 Application of the CVFEM for Magnetohydrodynamic Nanofluid Flow and Heat Transfer 180
5.3.1 Modeling Free Convection Between the Inclined Hot Roof of a Basement and a Cold Environment 180
5.3.2 Modeling Fluid Flow Due to Convective Heat Transfer from a Hot Pipe Buried in Soil 194
5.3.3 Natural Convection in an Inclined, L-Shaped, Porous Enclosure 200
References 209

Appendix A CVFEM Code for Lid Driven Cavity 211
Index 221

Nomenclature

A	amplitude
C_p	specific heat at a constant pressure
D_B	Brownian diffusion coefficient
D_T	thermophoretic diffusion coefficient
Gr_f	Grashof number
Ha	Hartmann number $\left(HB_x\sqrt{\sigma_f/\mu_f}\right)$
Le	Lewis number (α/D_B)
N	number of undulations
Nb	Brownian motion parameter $\left((\rho c)_p D_B(\phi_h-\phi_c)/(\rho c)_f\alpha\right)$
Nt	thermophoretic parameter $\left((\rho c)_p D_T(T_h-T_c)/\left[(\rho c)_f\alpha T_c\right]\right)$
Nu	Nusselt number
Nr	Buoyancy ratio $\left(\left(\rho_p-\rho_0\right)(\phi_h-\phi_c)/\left[(1-\phi_c)\rho_{f_0}\beta L(T_h-T_c)\right]\right)$
Pr	Prandtl number (υ_f/α_f)
J	electric current
T	fluid temperature
u,v	velocity components in the x-direction and y-direction
U,V	dimensionless velocity components in the X-direction and Y-direction
x,y	space coordinates
X,Y	dimensionless space coordinates
r	nondimensional radial distance
k	thermal conductivity
L	gap between inner and outer boundary of the enclosure $L=r_{out}-r_{in}$
$\vec{g}$	gravitational acceleration vector
Ra	Rayleigh number
q''	heat flux
Rd	radiation parameter

GREEK SYMBOLS

γ	angle measured from right plane
ζ	inclination angle
γ	angle of turn of the semiannulus enclosure
ε	eccentricity
α	thermal diffusivity
σ	electrical conductivity
ϕ	volume fraction
μ	dynamic viscosity
ω	vorticity
Ω	dimensionless vorticity
υ	kinematic viscosity
ψ	stream function

Ψ dimensionless stream function
Θ dimensionless temperature
ρ fluid density
β thermal expansion coefficient
μ_0 magnetic permeability of vacuum

SUBSCRIPTS

c cold
h hot
loc local
ave average
nf nanofluid
f base fluid
p solid particles
in inner
out outer

CHAPTER

Control volume finite element method (CVFEM) 1

1.1 INTRODUCTION

Fluid flow has several applications in engineering and nature. Mathematically, real flows are governed by a set of nonlinear partial differential equations in complex geometry. So, suitable solutions can be obtained through numerical techniques such as the finite difference method, the finite volume method (FVM), and the finite element method (FEM). In the past decade the FEM has been developed for use in the area of computational fluid dynamics; this method has now become a powerful method to simulate complex geometry. However, the FVM is applied most in calculating fluid flows. The control volume finite element method (CVFEM) combines interesting characteristics from both the FVM and FEM. The CVFEM was presented by Baliga and Patankar [1,2] using linear triangular finite elements and by Raw and Schneider [3] using linear quadrilateral elements. Several authors have improved the CVFEM from then to now. Raw et al. [4] applied a nine-nodded element to solve heat conduction problems. Banaszek [5] compared the Galerkin and CVFEM methods in diffusion problems using six-nodded and nine-nodded elements. Campos Silva et al. [6] developed a computational program using nine-nodded finite elements based on a control volume formulation to simulate two-dimensional transient, incompressible, viscous fluid flows. Campos Silva and Moura [7] and Campos Silva [8] presented results for fluid flow problems. The CVFEM combines the flexibility of FEMs to discretize complex geometry with the conservative formulation of the FVMs, in which the variables can be easily interpreted physically in terms of fluxes, forces, and sources. Saabas and Baliga [9,10] referenced a list of several works related to FVMs and CVFEMs. Voller [11] presented the application of CVFEM for fluids and solids. Sheikholeslami et al. [12] studied the problem of natural convection between a circular enclosure and a sinusoidal cylinder. They concluded that streamlines, isotherms, and the number, size, and formation of cells inside the enclosure strongly depend on the Rayleigh number, values of amplitude, and the number of undulations of the enclosure.

1.2 DISCRETIZATION: GRID, MESH, AND CLOUD

In general there are three ways to place node points into a domain [11].

1.2.1 GRID

A basic approach assigns the location of nodes using a structured grid where, in a two-dimensional domain, the location of a node is uniquely specified by a row and a column index (Fig. 1.1a). Although such a structured approach can lead to convenient and efficient discrete equations, it lacks flexibility in accommodating complex geometries or allowing for the local concentration of nodes in solution regions of particular interest.

1.2.2 MESH

Geometric flexibility, usually at the expense of solution efficiency, can be added by using an unstructured mesh. Figure 1.1b shows an unstructured mesh of triangular elements. In two-dimensional domains triangular meshes are good selections because they can tessellate any planar surface. Note, however, that other choices of elements can be used in place of or in addition to triangular elements. The mesh can be used to determine the placement of the nodes. A common choice is to place the nodes at the vertices of the elements. In the case of triangles this allows for the

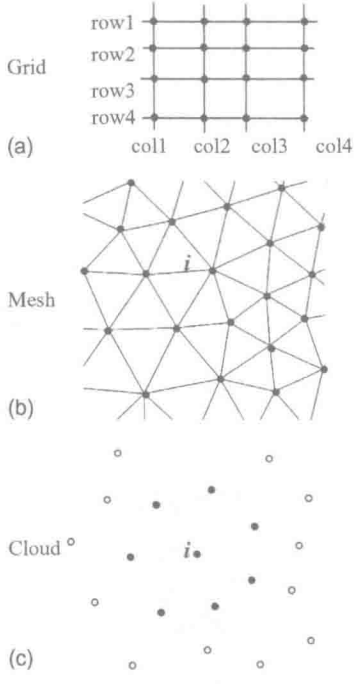

FIGURE 1.1

Different forms of discretization [11], including a grid (a), mesh (b), and cloud (c).

approximation of a dependent variable over the element, by linear interpolation between the vertex nodes. Higher-order approximations can be arrived by using more nodes (e.g., placing nodes at midpoints) or alternative elements (e.g., quadrilaterals). When considering an unstructured mesh recognizing the following is important:

1. The quality of the numerical solution obtained is critically dependent on the mesh. For example, avoiding highly acute angles is a key quality requirement for a mesh of triangular elements. The generation of appropriate meshes for a given domain is a complex topic worthy of a monograph in its own right. Fortunately, for two-dimensional problems in particular, there is a significant range of commercial and free software that can be used to generate quality meshes.
2. The term *unstructured* is used to indicate a lack of a global structure that relates the position of all the nodes in the domain. In practice, however, a local structure—the region of support—listing the nodes connected to a given node i is required. Establishing, storing, and using this local data structure is one of the critical ingredients in using an unstructured mesh.

1.2.3 CLOUD

The most flexible discretization is to simply populate the domain with node points that have no formal background grid or mesh connecting the nodes. Solution approaches based on this "meshless" form of discretization create local and structures, usually based on a "cloud" of neighboring nodes that fall within a given length scale of a given node i [13] (Fig. 1.1c).

1.3 ELEMENT AND INTERPOLATION SHAPE FUNCTIONS

A building block of discretization is the triangular element (Fig. 1.2). For linear triangular elements the node points are placed at the vertices. In Fig. 1.2, the nodes, moving in a counterclockwise direction, are labeled 1, 2, and 3. Values of the dependent variable ϕ are calculated and stored at these node points.

In this way, values at an arbitrary point (x, y) within the element can be approximated with linear interpolation

$$\phi \approx ax + by + c, \tag{1.1}$$

where the constant coefficients a, b, and c satisfy the nodal relationships

$$\phi_i = ax_i + by_i + c, \quad i = 1, 2, 3. \tag{1.2}$$

Equation (1.1) can be more conveniently written in terms of the shape function N_1, N_2, and N_3, where

$$N_i(x, y) = \begin{cases} 1 & \text{At node } i \\ 0 & \text{At all points on side opposite node } i \end{cases} \tag{1.3}$$

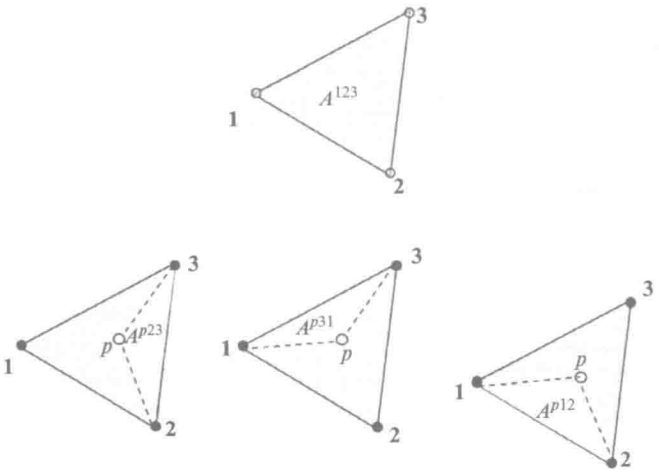

FIGURE 1.2

An element indicating the areas used in shape function definitions [11].

$$\sum_{i=1}^{3} N_i(x,y) = 1 \quad \text{At every point in the element} \tag{1.4}$$

such that, over the element the continuous unknown field can be expressed as the linear combination of the values at nodes $i = 1,2,3$:

$$\phi(x,y) \approx \sum_{i=1}^{3} N_i(x,y)\phi_i. \tag{1.5}$$

With linear triangular elements a straightforward geometric derivation for the shape functions can be obtained. With reference to Fig. 1.2, observe that the area of the element is given by

$$A^{123} = \frac{1}{2}\begin{vmatrix} 1 & x_1 & y_1 \\ 1 & x_1 & y_1 \\ 1 & x_1 & y_1 \end{vmatrix} = \frac{1}{2}[(x_2y_3 - x_3y_2) - x_1(y_3 - y_2) + y_1(x_3 - x_2)] \tag{1.6}$$

and the area of the subelements with vertices at points $(p,2,3)$, $(p,3,1)$, and $(p,1,2)$, where p is an arbitrary and variable point in the element, are given by

$$\begin{aligned} A^{p23} &= [(x_2y_3 - x_3y_2) - x_p(y_3 - y_2) + y_p(x_3 - x_2)] \\ A^{p31} &= [(x_3y_1 - x_1y_3) - x_p(y_1 - y_3) + y_p(x_1 - x_3)] \\ A^{p12} &= [(x_1y_2 - x_2y_1) - x_p(y_2 - y_1) + y_p(x_2 - x_1)] \end{aligned} \tag{1.7}$$

Based on these definitions, it follows that the shape functions are given by

$$N_1 = A^{P23}/A^{123}, \quad N_2 = A^{P31}/A^{123}, \quad N_3 = A^{P12}/A^{123}. \tag{1.8}$$

Note that, when point p coincides with node i $(1,2,\text{or}\,3)$, the shape function $N_i = 1$, and when point p is anywhere on the element side opposite node i, the associated subelement area is zero, and, through Eq. (1.8), the shape function $N_i = 0$. Hence

the shape functions defined by Eq. (1.8) satisfy the required condition in Eq. (1.3). Further, note that at any point p, the sum of the areas:

$$A^{P23} + A^{P31} + A^{P12} = A^{123} \tag{1.9}$$

is such that the shape functions at (x_p, y_p) sum to unity. Hence the shape functions defined by Eq. (1.8) also satisfy the conditions in Eq. (1.4). For future reference, it is worthwhile to note that the following constants are the derivatives of the shape functions in Eq. (1.8) over the element:

$$\begin{aligned} N_{1x} &= \frac{\partial N_1}{\partial x} = \frac{(y_2 - y_3)}{2A^{123}}, \quad N_{1y} = \frac{\partial N_1}{\partial y} = \frac{(x_2 - x_3)}{2A^{123}} \\ N_{2x} &= \frac{\partial N_2}{\partial x} = \frac{(y_3 - y_2)}{2A^{123}}, \quad N_{2y} = \frac{\partial N_2}{\partial y} = \frac{(x_1 - x_3)}{2A^{123}} \\ N_{3x} &= \frac{\partial N_3}{\partial x} = \frac{(y_1 - y_2)}{2A^{123}}, \quad N_{3y} = \frac{\partial N_3}{\partial x} = \frac{(x_2 - x_1)}{2A^{123}} \end{aligned} \tag{1.10}$$

1.4 REGION OF SUPPORT AND CONTROL VOLUME

The local structure on the mesh in Fig. 1.1b is defined in terms of the region of support—the list of nodes that share a common element with a given node i [11] (Fig. 1.3). In this region of support, as illustrated in Fig. 1.3, a control volume is created by joining the center of each element in the support to the midpoints of the

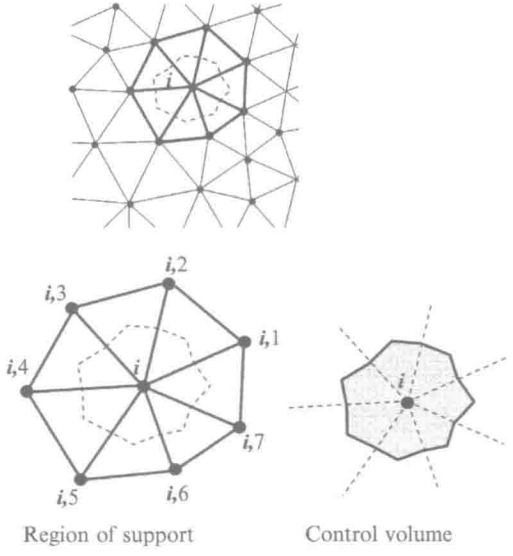

FIGURE 1.3

Region of support and control volume for node i in an unstructured mesh of linear triangular elements [11].

element sides that pass through node i. This creates a closed polygonal control volume with $2m$ sides (faces), where m is the number of elements in the support. Each element contributes one-third of its area to the control volume area, and the volumes from all the nodes tessellate the domain without overlapping.

1.5 DISCRETIZATION AND SOLUTION

1.5.1 STEADY-STATE ADVECTION-DIFFUSION WITH SOURCE TERMS

To illustrate a solution procedure using the CVFEM, one can consider the general form of advection-diffusion equation for node i in integral form:

$$-\int_V Q\,\mathrm{d}V - \int_A k\nabla\phi\cdot n\,\mathrm{d}A + \int_A (v\cdot n)\phi\,\mathrm{d}A = 0 \tag{1.11}$$

or point form

$$-\nabla\cdot(k\nabla\phi) + \nabla\cdot(v\phi) - Q = 0, \tag{1.12}$$

which can be represented by the system of CVFEM discrete equations as:

$$[a_i + Qc_i + Bc_i]\phi_i = \sum_{j=1}^{n_i} a_{i,j}\phi_{S_{i,j}} + Q_{B_i} + B_{B_i}. \tag{1.13}$$

In Eq. (1.13), the a's are the coefficients, the index (i, j) indicates the jth node in the support of node i, the index $S_{i,j}$ provides the node number of the jth node in the support, the Bs account for boundary conditions, and the Qs for source terms. For the selected triangular element shown in Fig. 1.4, this approximation (without considering the source term) leads to:

$$-\left(a_1^k + a_1^u\right)\phi_i + \left(a_2^k + a_2^u\right)\phi_{S_{i,3}} + \left(a_2^k + a_2^u\right)\phi_{S_{i,4}} = 0 \tag{1.14}$$

Using upwind method for advection coefficients identified by the superscript u, are given by

$$\begin{aligned} a_1^u &= \max\left[q_{f1}, 0\right] + \max\left[q_{f2}, 0\right] \\ a_2^u &= \max\left[-q_{f1}, 0\right] \\ a_3^u &= \max\left[-q_{f2}, 0\right] \end{aligned} \tag{1.15}$$

The diffusion coefficients, identified with the superscript k, are given by

$$\begin{aligned} a_1^k &= -k_{f1}N_{1x}\Delta\vec{y}_{f1} + k_{f1}N_{1y}\Delta\vec{x}_{f1} - k_{f2}N_{1x}\Delta\vec{y}_{f2} + k_{f2}N_{1y}\Delta\vec{x}_{f2} \\ a_2^k &= -k_{f1}N_{2x}\Delta\vec{y}_{f1} + k_{f1}N_{2y}\Delta\vec{x}_{f1} - k_{f2}N_{2x}\Delta\vec{y}_{f2} + k_{f2}N_{2y}\Delta\vec{x}_{f2} \\ a_2^k &= -k_{f1}N_{3x}\Delta\vec{y}_{f1} + k_{f1}N_{3y}\Delta\vec{x}_{f1} - k_{f2}N_{3x}\Delta\vec{y}_{f2} + k_{f2}N_{3y}\Delta\vec{x}_{f2} \end{aligned} \tag{1.16}$$

In Eq. (1.15), the volume flow across faces 1 and 2 in the direction of the outward normal is

$$\begin{aligned} q_{f1} &= v\cdot nA|_{f1} = v_x^{f1}\Delta\vec{y}_{f1} - v_y^{f1}\Delta\vec{y}_{f1} \\ q_{f2} &= v\cdot nA|_{f2} = v_x^{f2}\Delta\vec{y}_{f2} - v_y^{f2}\Delta\vec{y}_{f2} \end{aligned} \tag{1.17}$$

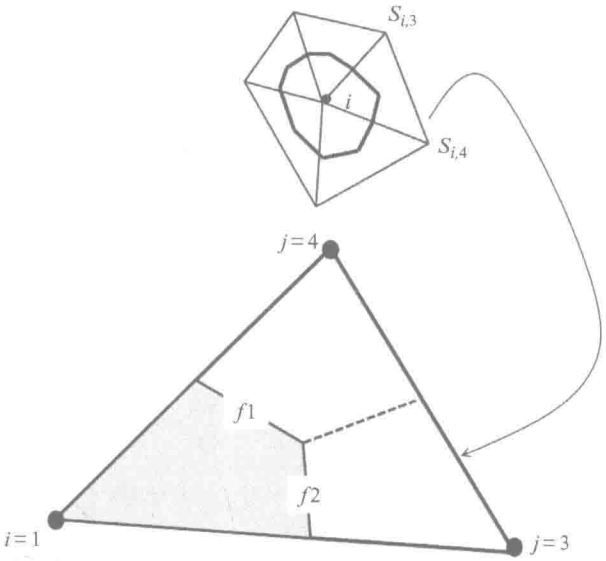

FIGURE 1.4

A sample triangular element and its corresponding control volume.

The value of the diffusivity at the midpoint of face 1 can be obtained as

$$k_{f1} = [N_1k_1 + N_2k_2 + N_3k_3]_{f1} = \frac{5}{12}k_1 + \frac{5}{12}k_2 + \frac{2}{12}k_3 \tag{1.18}$$

and at the midpoint of face 2 as

$$k_{f2} = [N_1k_1 + N_2k_2 + N_3k_3]_{f2} = \frac{5}{12}k_1 + \frac{2}{12}k_2 + \frac{5}{12}k_3. \tag{1.19}$$

The velocity component at the midpoint of face 1 is:

$$\begin{aligned} v_x^{f1} &= \frac{5}{12}v_{x_1} + \frac{5}{12}v_{x_2} + \frac{2}{12}v_{x_3} \\ v_y^{f1} &= \frac{5}{12}v_{y_1} + \frac{5}{12}v_{y_2} + \frac{2}{12}v_{y_3} \end{aligned} \tag{1.20}$$

On face 2 the velocity component is:

$$\begin{aligned} v_x^{f2} &= \frac{5}{12}v_{x_1} + \frac{2}{12}v_{x_2} + \frac{5}{12}v_{x_3} \\ v_y^{f2} &= \frac{5}{12}v_{y_1} + \frac{2}{12}v_{y_2} + \frac{5}{12}v_{y_3} \end{aligned} \tag{1.21}$$

These values can be used to update the ith support coefficients using the following equation:

$$\begin{aligned} a_i &= a_i + a_1^k \\ a_{i,3} &= a_{i,3} + a_2^k \\ a_{i,4} &= a_{i,4} + a_3^k \end{aligned} \tag{1.22}$$

In Eq. (1.16), moving counterclockwise around node i, the signed distances are:

$$\begin{aligned} \Delta\vec{x}_{f1} &= \frac{x_3}{3} - \frac{x_2}{6} - \frac{x_1}{6}, \quad \Delta\vec{x}_{f2} = -\frac{x_2}{3} + \frac{x_3}{6} + \frac{x_1}{6} \\ \Delta\vec{y}_{f1} &= \frac{y_3}{3} - \frac{y_2}{6} - \frac{y_1}{6}, \quad \Delta\vec{y}_{f2} = -\frac{y_2}{3} + \frac{y_3}{6} + \frac{y_1}{6} \end{aligned}, \tag{1.23}$$

the derivatives of the shape functions are:

$$\begin{aligned} N_{1x} &= \frac{\partial N_1}{\partial x} = \frac{(y_2 - y_3)}{2V^{\text{ele}}}, \quad N_{1y} = \frac{\partial N_1}{\partial y} = \frac{(x_3 - x_2)}{2V^{\text{ele}}} \\ N_{2x} &= \frac{\partial N_2}{\partial x} = \frac{(y_3 - y_1)}{2V^{\text{ele}}}, \quad N_{2y} = \frac{\partial N_1}{\partial y} = \frac{(x_1 - x_3)}{2V^{\text{ele}}}, \\ N_{3x} &= \frac{\partial N_2}{\partial x} = \frac{(y_1 - y_2)}{2V^{\text{ele}}}, \quad N_{3y} = \frac{\partial N_3}{\partial y} = \frac{(x_2 - x_1)}{2V^{\text{ele}}} \end{aligned} \tag{1.24}$$

and the volume of the element is

$$V^{\text{ele}} = \frac{(x_2 y_3 - x_3 y_2) + x_1(y_2 - y_3) + y_1(x_3 - x_2)}{2}. \tag{1.25}$$

The obtained algebraic equations from the discretization procedure using CVFEM are solved using the Gauss-Seidel method.

1.5.2 IMPLEMENTATION OF SOURCE TERMS AND BOUNDARY CONDITIONS

The boundary conditions for the present problem can be enforced using B_{B_i} and B_{C_i} as follows [14–16]:

$$\text{Insulated boundary:} \quad B_{B_i} = 0 \quad \text{and} \quad B_{C_i} = 0 \tag{1.26}$$

$$\text{Fixed value boundary:} \quad B_{B_i} = \phi_{\text{value}} \times 10^{16} \quad \text{and} \quad B_{C_i} = 10^{16} \tag{1.27}$$

$$\text{Fixed flux boundary:} \quad B_{B_i} = A_k \times q'' \quad \text{and} \quad B_{C_i} = 0 \tag{1.28}$$

where ϕ_{value} is the prescribed value on the boundary and A_k is the length of the control volume surface on the boundary segment.

To provide a general treatment for boundary conditions, some preliminary calculation of the boundary face areas associated with each node j in a given boundary segment is required. Figure 1.5 shows a schematic of the kth ($k = 3$) boundary, indicating the data structure. Assuming unit depth, the face area associated with any node j of the boundary segment highlighted in Fig. 1.5 is given by

$$A_{k,j} = \begin{cases} \text{Upper}_1 \\ \text{Upper}_j + \text{Lower}_j, \quad 2 \le j \le n_{B,k} - 1 \\ \text{Lower}_{n_{B,k}} \end{cases} \tag{1.29}$$